Experimental study of radiation damage of the plastic scintillators caused by radiation at IREN facility

S.V. Afanasiev[1,2], S.B. Borzakov[1,2], V.A. Egorov[1], I.A. Golutvin[1], Z.A. Igamkulov[1], A.I. Malakhov[1,2], P.V. Moisenz[1], V.G. Pyataev[1], P.V. Sedyshev[1], V.N. Shvetsov[1], V.A. Smirnov[1], A.O. Zontikov[1]

[1]*Joint Institute for Nuclear Research, Dubna, Russia*
[2]*University "Dubna", Dubna, Russia*

Abstract

This paper describes the studies of four types of plastic scintillator SCSN-81, UPS-923A (made in KIPT, Kharkov), BC-408, LHE (made in JINR, Dubna) performed by the CMS JINR group on Intense Resonance Neutron source (IREN) – the JINR neutron source facility. These studies were performed to measure a light yield from samples of different shapes before and after irradiation. The investigation was performed to understand the dependence of light yield on the dose rate.

1. Introduction

The hadron calorimeter (HCAL) of CMS uses a plastic scintillator SCSN-81 as detection media [1, 2]. The main weakness of plastic scintillators is time constraints to work in fields of high radiation. The HCAL TDR [3] studies of radiation damage of SCSN-81 have defined an opportunity of using the plastics during 10 years of its operation on LHC. The proposed reduction of light yield was up to 40% for the most loaded scintillators (the absorbed dose was ~6 Mrad). But the first three years of HCAL operation have shown the unpredictable decrease of light yields from plastic detectors (tiles) of the end-cup hadron calorimeter (HE). These tiles are composed from megatiles of first 5 layers with $\eta = 2.0 – 3.0$ [4]. It has become clear that some affections of radiation on plastic were not taken into account before. For example, it may be a radiation dose rate. Earlier investigations reported about significant (by two times) reduction of the light yield from SCSN-81 for small levels of the dose rate [5]. Some other unaccounted factors may also effect on degradation of the plastic detector.

This paper describes some studies of four types of plastic scintillator SCSN-81, UPS-923A (made in KIPT, Kharkov), BC-408, LHE (made in JINR, Dubna) performed by the CMS JINR group on Intense Resonance Neutron source (IREN) [6].

2. IREN – neutron and gamma source for test samples

The scientific research complex IREN is one of the JINR basic facilities. IREN is based on the electron linear accelerator and contains a neutron producing target. The achieved parameters are as follows: electron energy – up to 30 MeV; electron beam current – 5.0 μA; pulse width – 100 ns; repetition rate – 25 Hz; integral neutron yield $–2 \cdot 10^{11}$ n/cm^{2}s.

The material of the neutron producing target is a tungsten based alloy (W – 90%, Ni – 7%, Fe – 3%, density 17.2 g/cm^3). It is formed as a cylinder 40 mm in diameter and 100 mm height spaced within the aluminum can,140 mm in diameter and 140 mm

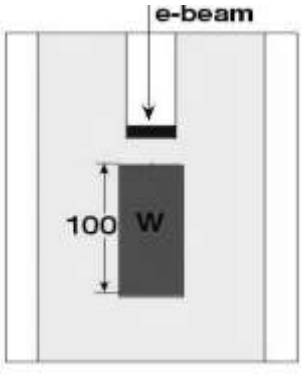

Figure 1. A sche-matic view of the neutron producing target.

height (see Figure 1). Distilled water is circulating inside the can to provide the target cooling and neutron moderation.

Figures 2 and 3 show neutron and gamma spectra calculated by means of FLUKA. The fluxes of secondary particles are determined on the distance of 9 cm from side surface of target and for mean value of electron beam current 3.85 μA with energy distribution of electrons shown in Figure 4.

The neutron spectrum of IREN is very close to the calculated neutron spectrum of HE CMS [7].

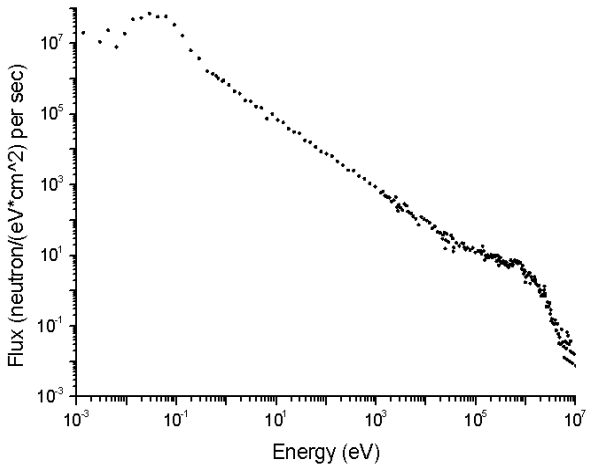

Figure 2. Calculated spectra of neutrons for IREN.

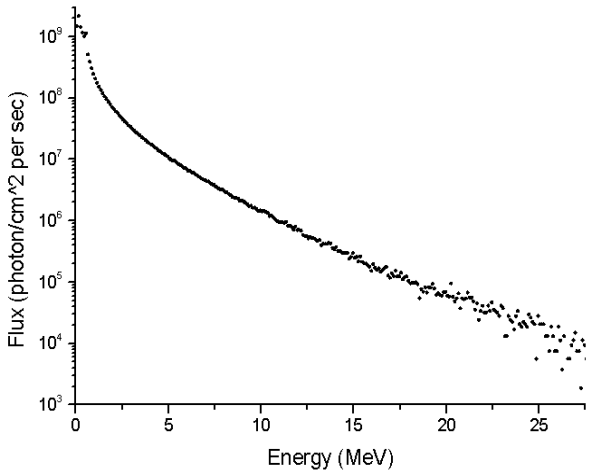

Figure 3. Calculated spectra of gammas for IREN.

Figure 5 shows the gradient distribution of the radiation field around the IREN target formed per one electron from Linac.

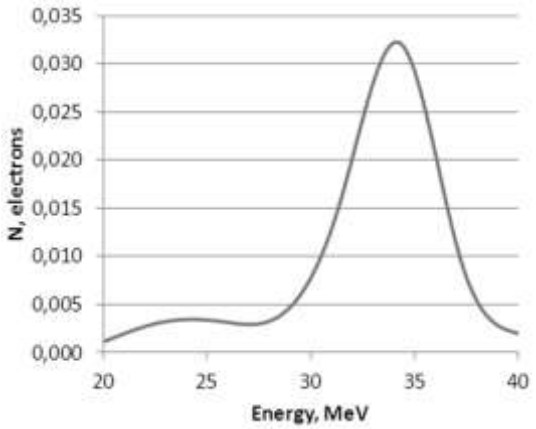

Figure 4. Energy distribution of primary electrons for $2.403 \cdot 10^{13}$ electron/s.

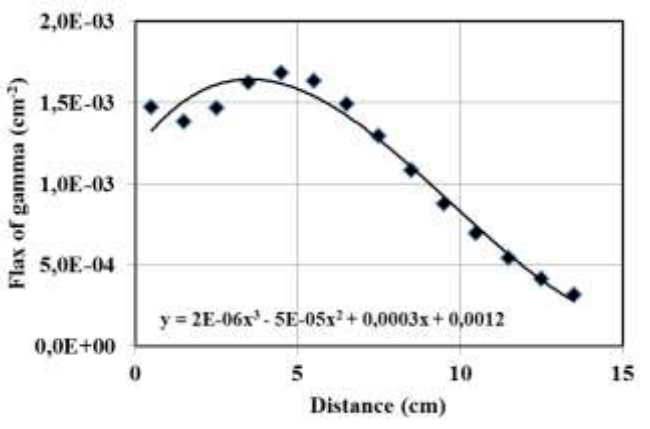

Figure 5. Distribution of gamma of all energies vs. distance along the target side. Gammas have energy more than 100 keV.

The total neutron flux is $7.3 \cdot 10^{-6}$ cm^{-2} per one electron from Linac.
The total gamma flux is $1.3 \cdot 10^{-3}$ cm^{-2} per electron from Linac.

3. Irradiation program

The scintillator samples of three different shapes were prepared for the irradiation study:

- Sigma tiles, which are close to tile #27 in the layer #1 [8] with WLS Y11 d=0.85mm. It should help to understand SCSI-81/Y11 radiation damage as for 30 fb^{-1} integrated luminosity of CMS on LHC and predict the properties of HE tiles up to 500–700 fb^{-1}.

- Finger type scintillators: length 60 ÷ 148mm, width 12 ÷ 20mm, thickness 4mm. It will allow one to predict the radiation damage of the stripped tiles made from SCSN-81 and UPS-923A up to 2500 – 3000 fb^{-1} of the integrated luminosity.

- Square type samples 25 × 25 mm^2 made from SCSN-81, UPS-923A, BC-408 and LHE.

The thickness of all samples is 4mm. All the samples to prevent the damage of their surface were placed in individual paper boxes. Together with the sample we placed a film dosimeter FWT-60-00 (thickness 42.5 mkm) produced by West Technology. The dosimeters were placed in opaque envelopes to protect them against ultraviolet radiation.

The main idea of study is to measure the light yields of irradiated samples for several values of the dose rate and predict the light yield from the tiles of the current CMS setup (see Fig. 6) by using the experimental data.

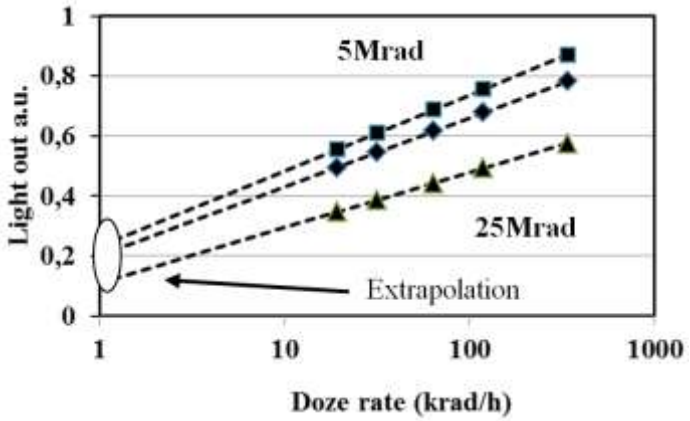

Figure 6. Extrapolation of experimental data to estimate the dose rate near 1 krad/h.

The samples are intended to expose with different dose rates from 0.00025 up to 0.338 Mrad/hr. The duration of measurements should take 90 days. The program of irradiation is as follows:

- "Sigma" tiles up to the dose of 0.3 Mrad – for understanding the SCSN-81/Y11 radiation

- damage for 30 fb^{-1} of the integrated luminosity;

- "Sigma" tiles up to the dose of 5.0 Mrad – for predicting the properties of the existing tiles up to 500 –700 fb^{-1};

- "Finger" type tiles up to the dose of 25 Mrad – for predicting the radiation damage of the new stripped tiles up to 2500 –3000 fb^{-1} of the integrated luminosity;

- "Squares" samples up to the dose of 25 Mrad – for understanding the properties of scintillators as function of the dose rate and the integrated dose.

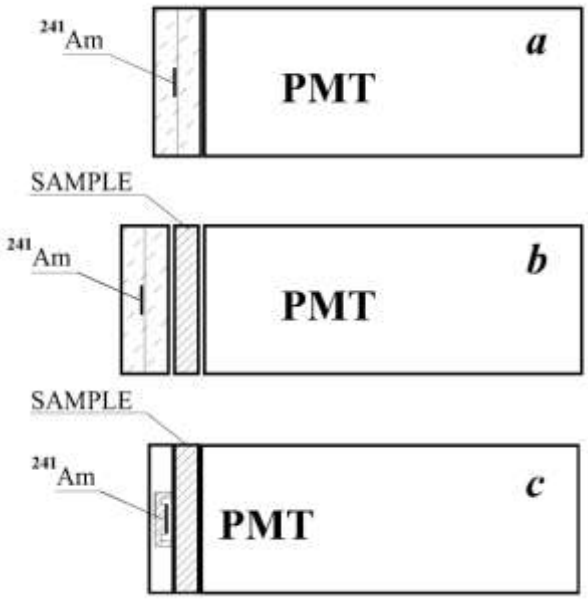

Figure 7. The devices to measure light transmission in the sample and degradation of scintillating emission.

Preliminary measurements of the light yield from all samples before their irradiation on IREN were carried out. A reference scintillator SCSN-81 (RS-Am) with ^{241}Am (source of α-particles with energy 5.637 MeV) mounted inside was used (see Figure 7d). The first step of testing was measuring of the light from RS-Am (see Figure 7a). The second step was a measurement of light transmission in a sample (see Figure 7b). The third step was measuring of the light yield from the sample. Figure 7c demonstrates the α-source (see Figure 7e) used for exiting the light in the sample. Those sets of measurements allow one to determine the light transmission in the sample and degradation of scintillating emission.

The sequence of operations while measuring the sample was as follows:

- The first measurement starts after equipment warming (about 30 minutes). It is a mesurement of the amplitude distribution from RS-Am. The mean value of the amplitude distribution is used to correct the following measurements.
- A measurement of ADC pedestal value.
- A measurement of the light losses in a sample (see Figure 7b). The reference light comes from RS-Am which is installed in front of a sample. The spectrum of the light passing through the sample SCSN-81 will be identical to the scintillation light. The remaining 3 types of scintillators UPS-923A, BC-408, LHE have the spectrum which is very close to the spectrum of RS-Am.
- A measurement of signals directly from a sample. The open α-source ^{241}Am is used (see Figure 7e). The α-source was always positioned in the same place for all the measured samples. The distance between the source and the sample was 0.2mm.
- The measurements of the amplitude distribution from RS-Am and ADC pedestal value at the end of a set of measurements were carried out.

The amplitude spectrum from the α-source emitting mono energetic particles looks very nice (pure Gaussian distribution). The amplitude distribution is shown in Figure 8.

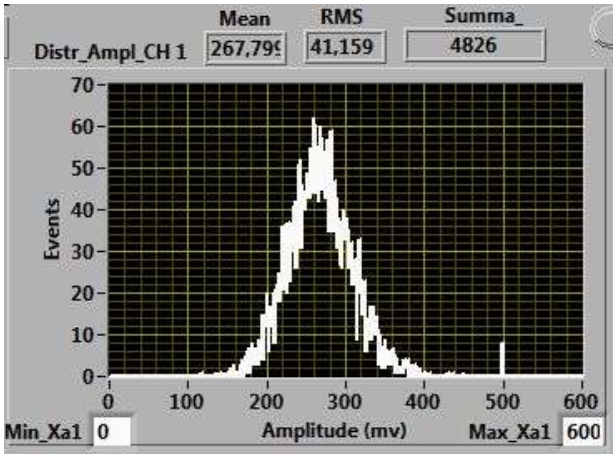

Figure 8. Amplitude distribution of signals from α-source.

Figure 9 shows a schematic view of the relative position of the target and single sample **S**, which allows one to define the dose rate of the sample taking into account the gamma flux going through each surface unit of the target.

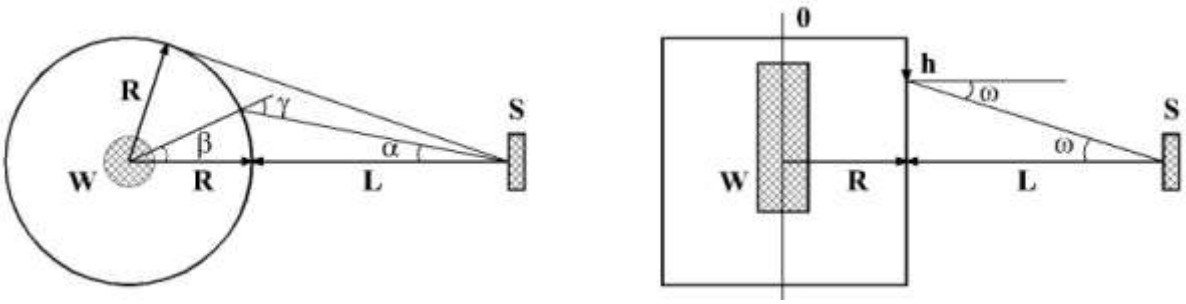

Figure 9. Schematic view of the sample position.

Figures 10 and 11 show the calculated flux of gammas through the surface of the sample in dependence on its position relative to the target. The surfaces of the samples are parallel to the cylindrical side of the target, which is located vertically.

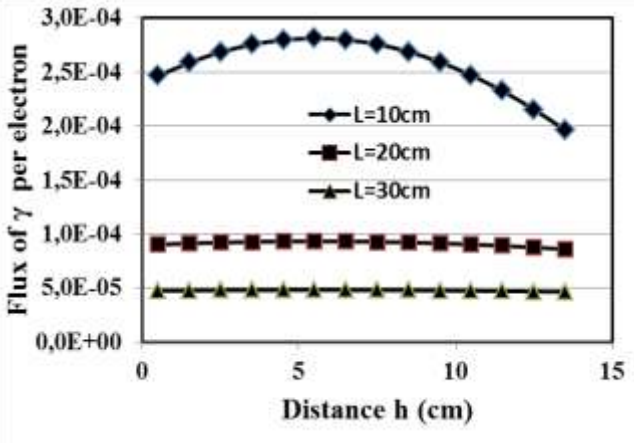

Figure 10. Dependence of the gamma flux per unit of the sample area on the vertical position of the sample relatively the upper edge of the target.

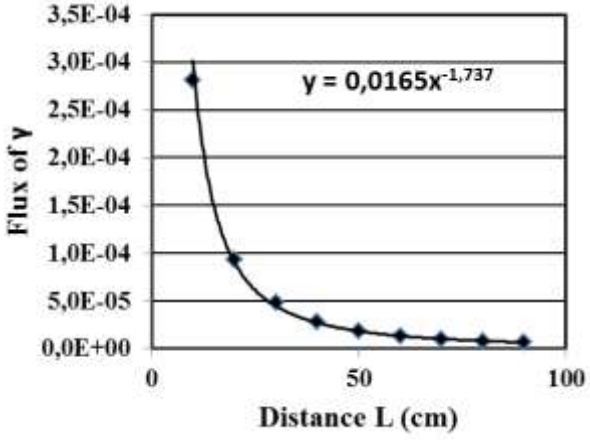

Figure 11. Dependence of the gamma flux per unit area of the sample on distance L between the target and the sample (vertical position of the sample h = 5 cm).

The calculated spectra of gamma rays and neutrons are shown in Tables 1 and 2. The exit secondary particles are normalized to the flux of primary electrons.

Table 1 contains the information about gamma fluxes (# of gammas·cm^{-2} per primary electron) going through the lateral surface of the target for several energy intervals. Value z determines the distance interval from the upper edge of the target. Gammas with energies below 100 keV were not considered.

Table 1. **The gamma fluxes through the lateral surface of the target.**

z, см	**Energy interval, MeV**				
	[0.1;3]	[3;10]	[10;20]	[20;30]	Total
[0;1]	1.3367E-03	1.2617E-04	6.5434E-06	1.1915E-07	1.4695E-03
[1;2]	1.2529E-03	1.2138E-04	6.1833E-06	1.1027E-07	1.3806E-03
[2;3]	1.3164E-03	1.4154E-04	6.8293E-06	8.3215E-08	1.4649E-03
[3;4]	1.4352E-03	1.7557E-04	1.0010E-05	1.2710E-07	1.6209E-03
[4;5]	1.4672E-03	2.0135E-04	1.3134E-05	1.8507E-07	1.6819E-03
[5;6]	1.4011E-03	2.1414E-04	1.5579E-05	2.3575E-07	1.6311E-03
[6;7]	1.2600E-03	2.1196E-04	1.7168E-05	2.9212E-07	1.4894E-03
[7;8]	1.0770E-03	1.9917E-04	1.7433E-05	3.2966E-07	1.2939E-03
[8;9]	8.8430E-04	1.7815E-04	1.6658E-05	3.7170E-07	1.0795E-03
[9;10]	7.0560E-04	1.5376E-04	1.4811E-05	3.5265E-07	8.7453E-04
[10;11]	5.5058E-04	1.2977E-04	1.3050E-05	3.6019E-07	6.9376E-04
[11;12]	4.2200E-04	1.0653E-04	1.0923E-05	3.3446E-07	5.3979E-04
[12;13]	3.1930E-04	8.6793E-05	8.8508E-06	2.8511E-07	4.1523E-04
[13;14]	2.3836E-04	6.9199E-05	7.2159E-06	2.5442E-07	3.1503E-04

Table 2 contains the information about neutron fluxes going through the lateral surface of the target for thermal neutrons (0.025 – 0.625 eV), epithermal neutrons (0.625 eV – 111 keV) and fast neutrons (111 keV – 20 MeV). The fluxes in Thermal, Epithermal, Fast columns are measured as # of neutrons·cm^{-2} per primary electron. The fluxes in Epithermal at 1eV/α column are measured as # of neutrons·cm^{-2}·eV^{-1} per primary electron.

Table 2. **The neutron fluxes going through the lateral surface of the target.**

z, см	Thermal	Epithermal	Epithermal at 1 eV/α	Fast	Total
[0;1]	6.0588E-07	1.6495E-06	9.7910E-08/ 0.9476	1.9992E-06	4.2545E-06
[1;2]	1.1386E-06	2.4654E-06	1.4620E-07 / 0.9500	2.5375E-06	6.1415E-06
[2;3]	1.4593E-06	2.9046E-06	1.7730E-07 / 0.9546	2.8512E-06	7.2151E-06
[3;4]	1.6265E-06	3.0371E-06	1.8940E-07 / 0.9556	2.9116E-06	7.5752E-06
[4;5]	1.6303E-06	2.8957E-06	1.8320E-07 / 0.9570	2.7330E-06	7.2590E-06
[5;6]	1.5592E-06	2.5935E-06	1.6920E-07 /0.9656	2.3764E-06	6.5292E-06
[6;7]	1.3870E-06	2.1644E-06	1.4700E-07 / 0.9697	1.9088E-06	5.4602E-06
[7;8]	1.1931E-06	1.7449E-06	1.2170E-07 / 0.9798	1.4777E-06	4.4158E-06
[8;9]	9.9379E-07	1.3372E-06	9.5720E-08 / 0.9828	1.0863E-06	3.4173E-06
[9;10]	7.9336E-07	9.9334E-07	7.6080E-08 / 0.9909	7.8567E-07	2.5724E-06
[10;11]	5.9753E-07	7.1168E-07	5.1700E-08 / 0.9922	5.5629E-07	1.8655E-06
[11;12]	4.3220E-07	4.9851E-07	4.3480E-08 / 1.0028	3.8072E-07	1.3114E-06
[12;13]	2.8113E-07	3.3305E-07	2.4570E-08 / 0.9974	2.5794E-07	8.7211E-07
[13;14]	1.3490E-07	1.9372E-07	1.2790E-08 / 1.0040	1.6787E-07	4.9646E-07

Figure 12 demonstrates the allocation of the samples near the target. Each sample that had been previously tested was placed in a paper box with film dosimeter FWT-60-00 covered by a lightproof shell. The box with the sample was labeled. Dosimeter readings and measurements of scintillator transparency were performed after 10-14 days, when their activation was reduced up to the level of the background radiation.

Figure 12. Sample allocation around the target.

4. A setup for measuring the light yield from the sample

The light yield from all the non-irradiated and irradiated samples was measured. Figure 13 shows a schematic view of the setup to measure the light yield from the sample. DRS4 is a four channel ADC from Paul Scherrer Institute (PSI), Switzerland, which is connected with PC controlled by OS Windows-7. LabView of National Instruments was used for data analysis. The interactive panel to operate with the experimental data coming from DRS4 is presented in Figure 14.

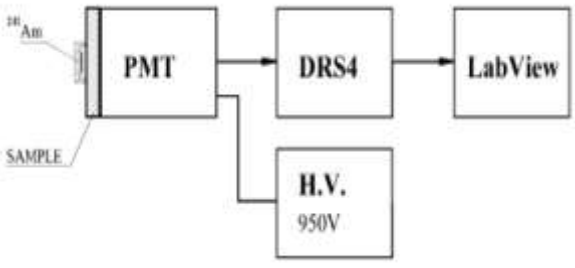

Figure 13. Schematic view of the setup to measure the light yield from the sample.

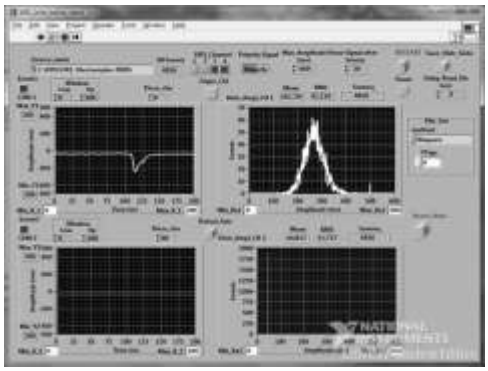

Figure 14. Interactive panel to operate with the experimental data analysis.

5. Experimental results

The first set of results has been received from the measurements of light outputs from the irradiated samples (25 × 25 mm^2) exposed to different absorbed doses. Figure 15 shows the results for scintillators SCSN-81, BC-408, UPS-923A and LHE.

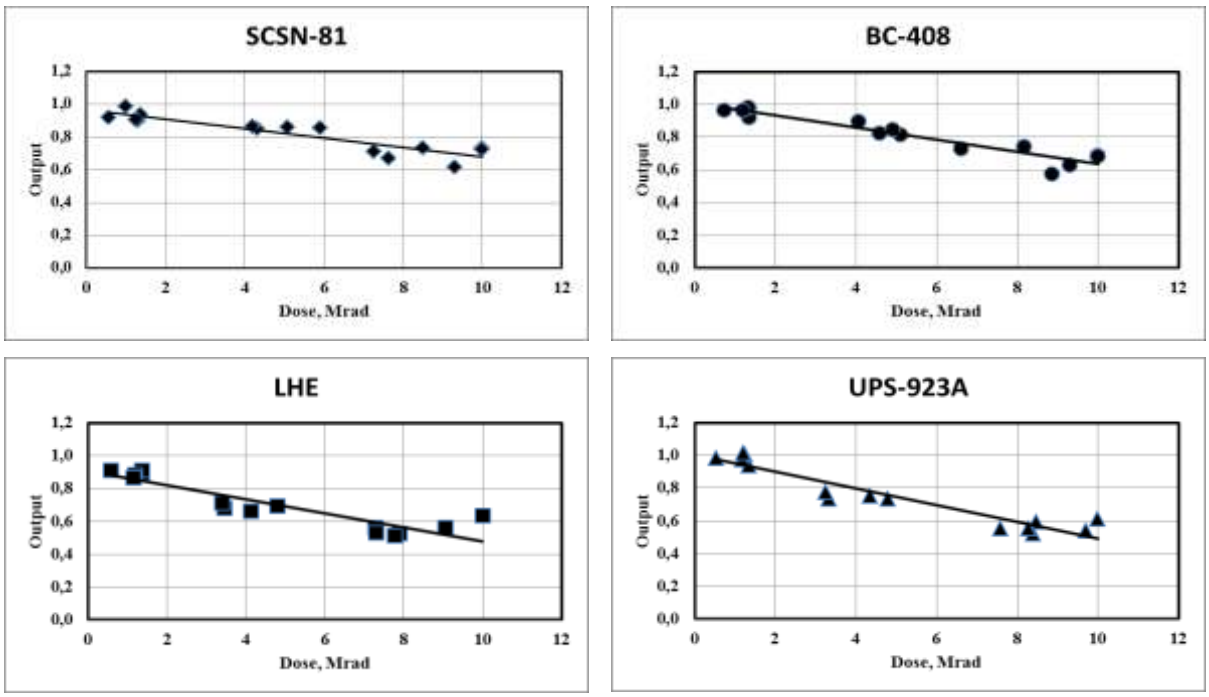

Figure 15. The distributions of light outputs from the irradiated samples normalized for the light measured before exposure vs. the total absorbed dose.

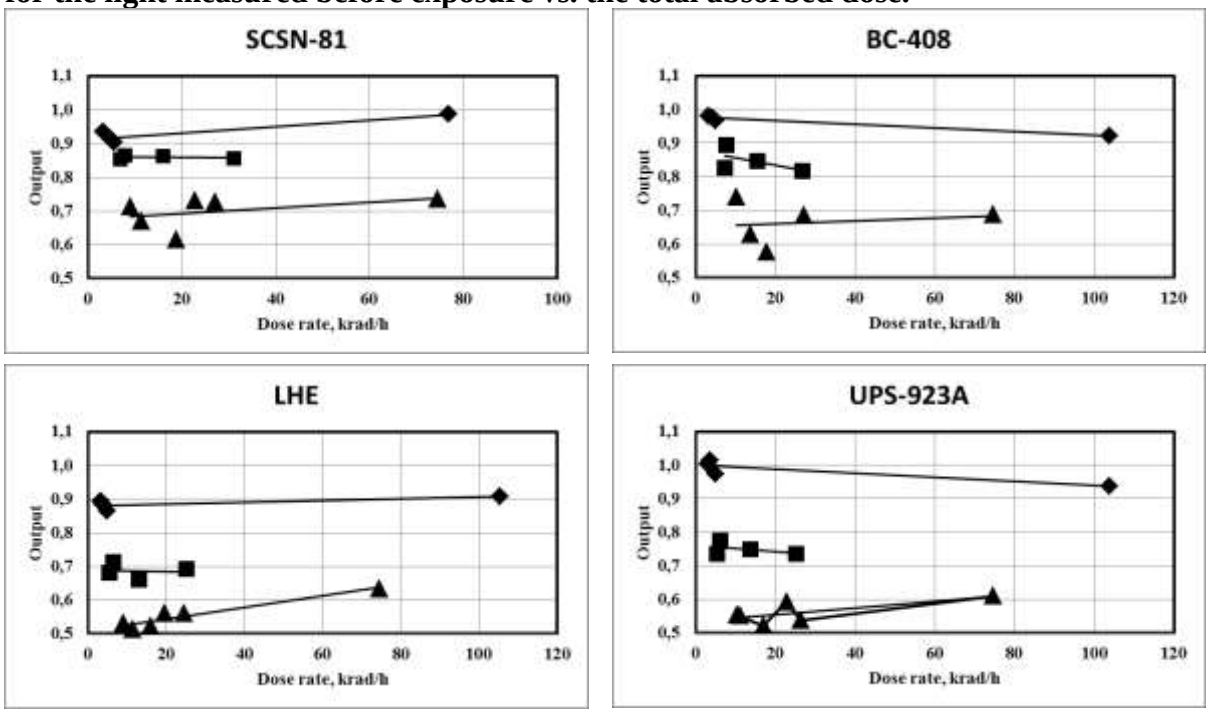

Figure 16. Dependence of relative light outputs on the dose rate values separately for each type of the investigated scintillators.

The absorbed dose in each sample was obtained from a reading of the film dosimeter. It should be noted that the measured values are very close to the dose calculation performed in advance. It will be observed that the points on all four graphics belong to three groups of the dose in the following ranges: 1÷1.4, 3.6÷4.8, 7.3÷10 Mrad. Each group contains the points with values of different dose rates starting from 2 krad/h up to ~ 100 krad/h.

Figure 16 shows the dependencies of relative light outputs vs. the dose rate values separately for each type of the investigated scintillators (25 × 25 mm^2). There is no confident evidence of considerable changes in the light outputs for different dose rates.

Figure 17 shows the dependence of relative light yield for samples of Sigma type. Table 3 presents the sizes of different samples used for testing.

Table 3. The sizes of Sigma type samples.

Name	S1	S2	S3	S4	S5	S6	S7	S8
Size mm^2	92-113x117	100-120x125	90-110x117	70-90x120	75-98x127	120-140x120	79-103x135	103-132x130

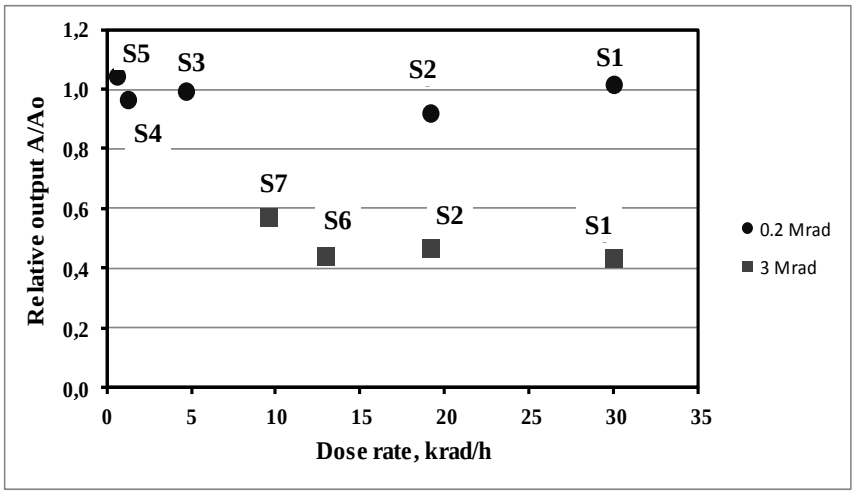

There are two groups of points corresponding to the absorbed doses 0.2 Mrad (circles) and 3.0 Mrad (squares) with different values of the dose rate inside them. There is no confident evidence of changes in the light outputs for different dose rates either.

Figure 17. Dependence of light yield for Sigma type samples.

The third set of more interesting results is received from the measurements of light outputs from the irradiated finger type scintillators (60 × 12 × 4 mm^3) exposed to different absorbed doses. The values of absorbed dose for SCSN-81 samples are laying in three groups of dose lying in the ranges: 4.8 – 5.5 Mrad, 6.9 – 10 Mrad and 13.4 – 24.7 Mrad. The absorbed doses of UPS-923A samples are laying only in one dose interval 13.4–20.3 Mrad. The absorbed dose in each sample was obtained from a reading of the film dosimeter. Each group contains points with values of the different dose rates starting from 2 krad/h up to ~ 100 krad/h.

Irradiated samples were incubated for at least 30 days to stabilize the parameters. Cosmic rays are used for measurement of light yield. Measurement scheme is shown in Fig. 18. This method allows to reconstruct almost the real state of formation and collection of light in the scintillator.

The obtained results are shown in Fig. 19 and 20. Figure 19 represented amplitude of the detected signal from the test sample, which is proportional to light yield, vs. the absorbed

dose. This amplitude is normalized to the amplitude of signal from the non-irradiated sample. Data for SCSN-81 were fitted by an exponential function. Figure 20 shows the dependencies of normalized amplitude vs. a dose rate separately for each type of scintillator and for each group of the closely adjacent absorbed dose intervals.

Again there is no confident evidence of changes in light output with different dose rates.

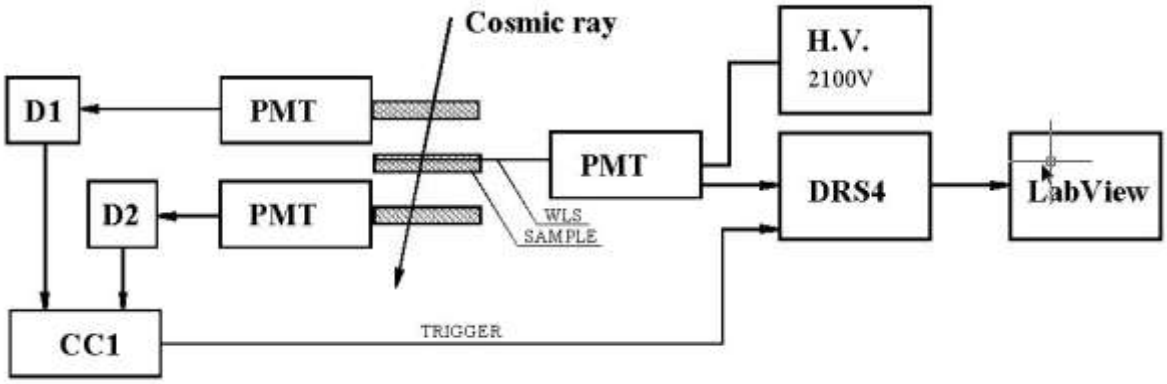

Figure 18. Scheme for measuring the parameters of finger type scintillators.

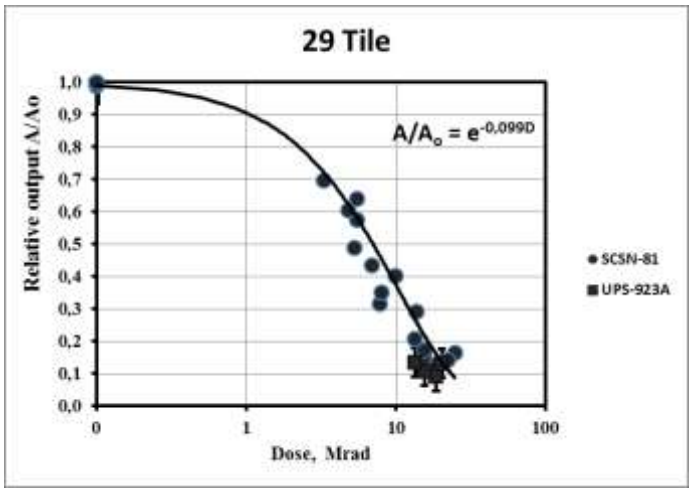

Figure 19. Dependence of normalized amplitude vs. an absorbed dose for finger type scintillators.

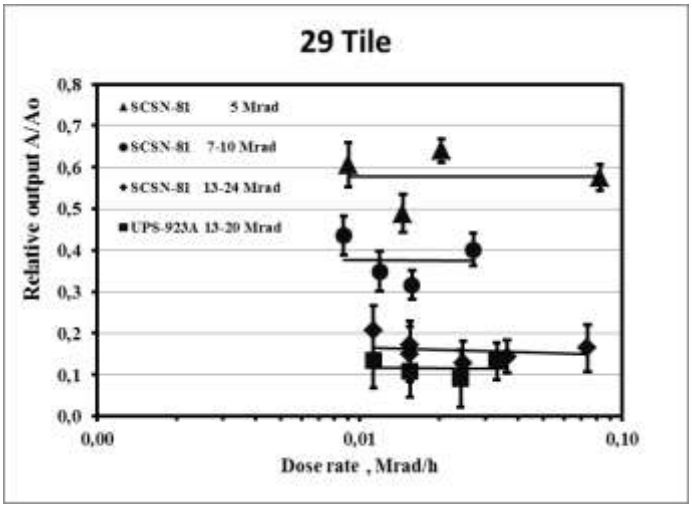

Figure 20. Dependencies of normalized amplitude vs. a dose rate separately for each type of finger type scintillator and for each group of the closely adjacent absorbed dose intervals.

6. Effect of induced radioactivity on a sample

In reality a HCAL scintillator is placed inside the brass absorber and receives the additional radioactivity emitted by radioisotopes induced in brass. The main source of producing radioisotopes is neutrons. Figure 21 shows a schematic view of the setup prepared for studying the induced radioactivity on the scintillator sample made from SCSN-81.

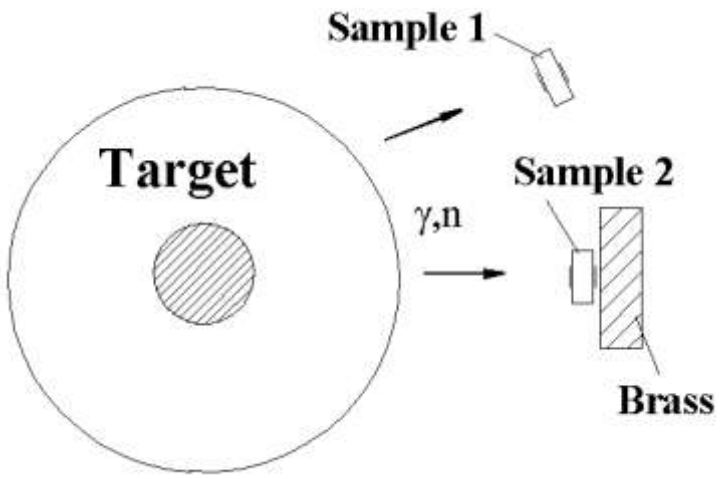

Figure 21. Setup to study the influence of induced radioactivity on a sample.

Two equal square samples (Sample1 and Sample2) are located at the same distance from the target. But behind Sample 2 and very close to it there is a brass disc with the following dimensions: diameter = 59mm, thickness = 9.6mm. The both samples were placed in individual paper boxes. From the front and the back of each sample there were two film dosimeters FWT-60-00. The dosimeters were placed in opaque envelopes to protect them against ultraviolet radiation.

The samples were exposed during 7.2 days. The calculated neutron flux going through the samples was $5.5 \cdot 10^{7}$ neutrons per second. The total flux was $3.4 \cdot 10^{13}$ neutrons.

The results of measurements are shown in Table 4. The values of the light yield from the front and back sides of the both samples were measured before and after exposure. The table shows the relative values of the light yields from the both sides of each sample.

Table 4. The results of influence of the induced radioactivity on a sample.

	Dose value from film dosimeters		***Relative light yield***	
	front side	**back side**	**front side**	**back side**
Sample 1	**6.7 Mrad**	**6.0 Mrad**	**0.85**	**0.86**
Sample 2	**9.0 Mrad**	**19.5 Mrad**	**0.82**	**0.79**

The dose absorbed by the film dosimeter from the front side of Sample 1 is slightly bigger than the dose from the back side. It is true because the incident radiation is reduced after passing through the scintillator. The measurements of the relative light yields from the both sides have confirmed it. The back side of the sample is damaged slightly less than from the front side. Figure 22 shows the consistency of the current (rose circle) and previous results of the relative light yield (see Figure 15 for SCSN-81) for Sample1.

The results of the relative light outputs from the both sides of Sample-2 have shown that radiation exposure of the back side is bigger than of the front side. It means that the sample feels the presence of additional radiation coming from the brass disc even for not very big

levels of neutron radiation. Some strange result of the dose measurement by the film dosimeter placed from the back side of Sample-2 may be explained by the presence of the radiation which is fully stopped in the dosimeter without reaching the sample.

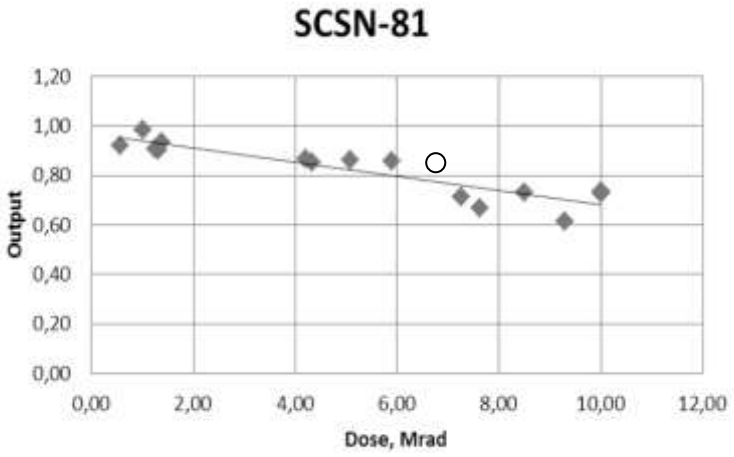

Figure 22. Consistency of the current and previous results.

The simulation by means of FLUKA was performed simultaneously with the experimental investigations of the influence of induced radioactivity on a sample. Figure 23 shows a schematic of the setup used for simulation.

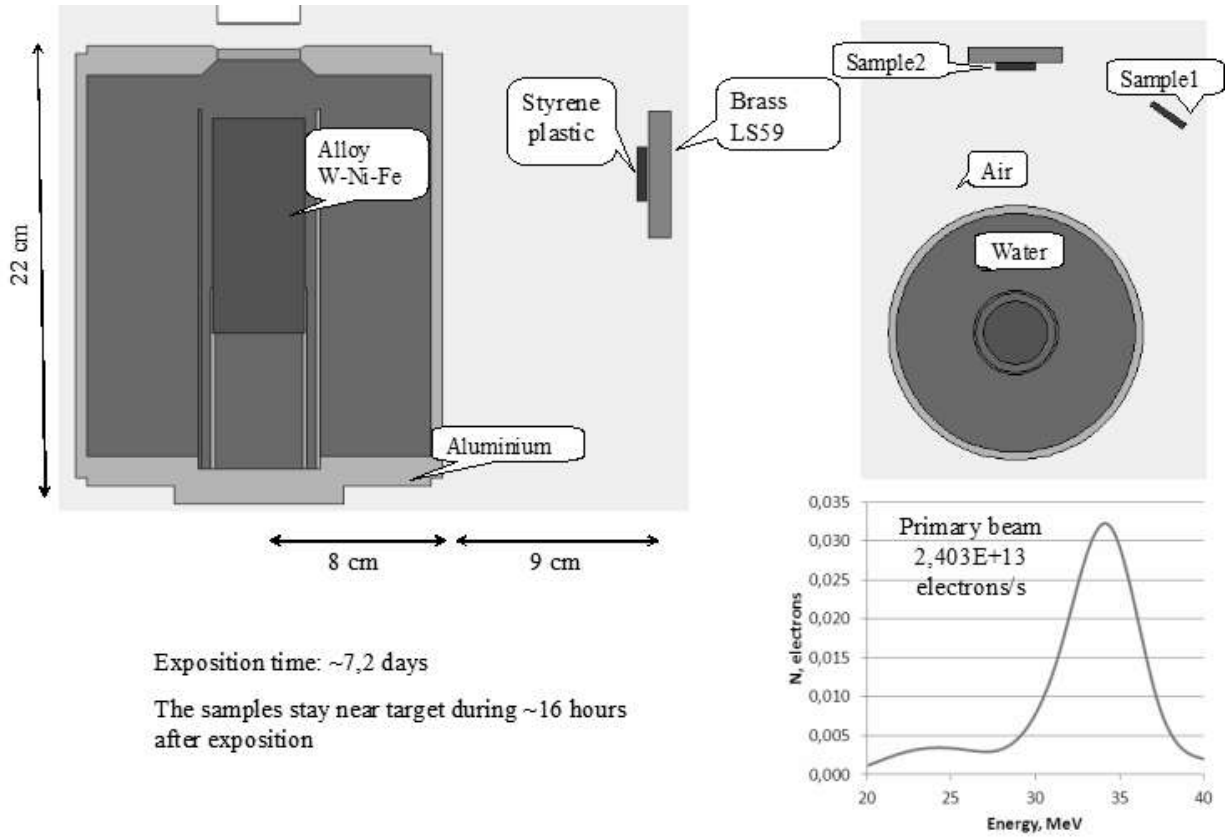

Figure 23. Schematic of the setup used for simulation.

The results of the simulation are given in Figure 24.

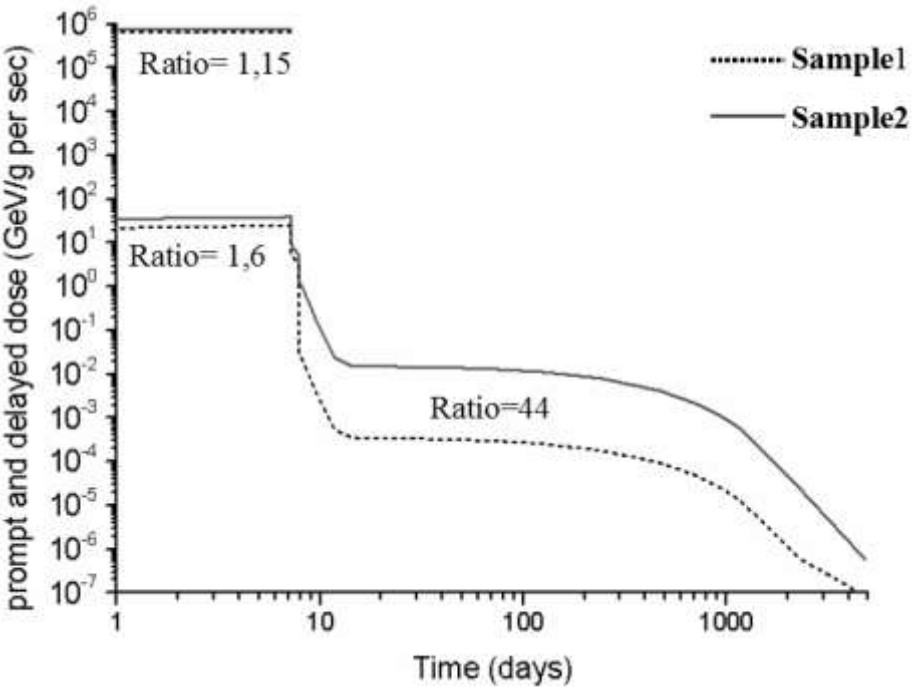

Figure 24. Results of the simulation of the induced radioactivity influence on a scintillator sample obtained by means of FLUKA.

The results may be divided in two regions. The first region shows the prompt dose absorbed by the both samples during the beam time. The second region shows a delayed dose absorbed by both samples during the irradiation and after it. Here, the delayed dose is a dose induced by decay radiation of residual nucleus which were build up in the target material and brass disc during the beam time.

The prompt dose absorbed during 7.2 days
for Sample1 is 4.065E+11 GeV/g ±0,57% (6.512 Mrad);
for Sample2 it is 4.693E+11 GeV/g ±0,53% (7.518 Mrad).
The delayed dose absorbed during the 7.2 days of irradiation and 13.2 years after it.
for Sample1 is 1.480E+07 GeV/g ±8.76% (237 rad);
for Sample2 it is 2.414E+07 GeV/g ±6.20% (387 rad).
The experimental and simulation results are in good agreement.

7. Conclusions

The studies of four types of plastic scintillator SCSN-81, UPS-923A (made in KIPT, Kharkov), BC-408, LHE (made in JINR, Dubna) were carried out by the CMS JINR group on Intense Resonance Neutron source (IREN) – the JINR neutron source facility. IREN is based on the electron linear accelerator (~30 MeV) and contains a neutron producing target. The total neutron flux is $7.3 \cdot 10^{-6}$ cm^{-2} per one electron of Linac. The total gamma flux is $1.3 \cdot 10^{-3}$ cm^{-2} per electron.

The scintillator samples of three different shapes were prepared to study the influence of irradiation. The thickness of all samples is 4mm. All samples, to prevent the damage of their surface, were placed in individual paper boxes. A film dosimeter FWT-60-00 (thickness 42.5mkm) produced by West Technology was placed together with the sample. Dosimeter reading was very close to the calculated data.

The first set of the experimental data was received from the measurements of light outputs from the irradiated square samples (25 × 25 mm^2) exposed to different total absorbed doses (1÷1.4, 3.6÷4.8, 7.3÷10 Mrad) with different values of different dose rate starting from 2 krad/h up to ~ 100 krad/h. The values of the absorbed dose in each sample were obtained from the reading of the film dosimeter. The results have not shown the confident evidences of some considerable changes in light outputs for different dose rates for all four types of the scintillator. The second set of the data was received from the exposure of Sigma type samples. No confident evidences of changes in the light outputs for different dose rates were found either. The influence of the additional radioactivity emitted by radioisotopes induced in the brass was also studied. The main source of producing radioisotopes is the neutrons. Two equal square samples (SCSN-81) were located at the same distance from the target. But behind one of them there was a brass disc (D = 59mm, thickness = 9.6mm). The samples were exposed during 7.2 days. The total flux of neutrons was $3.4 \cdot 10^{13}$. The results of the relative light outputs from the samples have shown the presence of additional radiation coming from the brass disc. Almost the same result of influence of induced radioactivity has been obtained from the simulation performed by means of FLUKA.

The authors express special thanks to the staff of Intense Resonance Neutron source (IREN) for active participation in the measurements. Many thanks are expressed to the group of engineers and scientists (A.P. Sumbaev, V.Ph. Minashkin, Yu. Becher, V.V. Kobec, V.G. Shabratov) providing the operation of IREN during the upgrade process.

References

1. CMS Collaboration. “The CMS Experiment at the CERN LHC“, 2008 J. Inst. 3 S08004, DOI: 10.1088/1748-0221/3/08/S08004.
2. CMS Collaboration. “Performance of the CMS hadron calorimeter with cosmic ray muons and LHC beam data”, 2010 J. Inst. **5** T03012, DOI: 10.1088/1748-0221/5/03/T03012, arXiv:0911.4991.
3. CMS collaboration. “CMS, the Hadron Calorimeter Technical Design Report,” CERN/LHCC 97-31 CMS TDR 2 (June 1997).
4. Pawel de Barbaro. HCAL Upgrades. CMS Upgrade Week, Karlsruhe, March-31-2014.
5. E. Biagtan, E. Goldberg, J. Harmon and R. Stephens. Effect of gamma radiation dose rate on the light output of commercial polymer scintillators. Nuclear Instruments and Methods in Physics Research, B **93**(1994)296-301.
6. IREN Facility http://flnp.jinr.ru/35/.
7. CMS HCAL Collaboration.” Design, Performance, and Calibration of CMS Hadron Endcap Calorimeters”, CMS-NOTE-2008-010, 32 p.
8. S.V. Afanasiev, P. de Barbaro, I.A. Golutvin et al. "Improvement of radiation hardness of the sampling calorimeters based on plastic scintillators", Nuclear Instruments and Methods in Physics Research A **717** (2013)11–13.